Elementary Magnetic Attitude Control System

A. Craig Stickler*
ITHACO, Inc., Ithaca, N.Y.
and
K.T. Alfriend†
Naval Research Laboratory, Washington, D.C.

A three-axis closed-loop attitude control system for Earth observatory momentum bias spacecraft is proposed. A horizon scanner and magnetometer are employed to measure attitude errors; no yaw sensor is required. Appropriate control signals are generated and used to command variable strength electromagnets, which interact with the geomagnetic field to reduce observed errors. This system provides for initial acquisition, precession control, nutation damping, and pitch axis momentum control. All functions are performed autonomously—no ground station interaction is required. Analytical expressions predicting system response are compared with numerical solutions of the governing equations, and with the results of the application of Floquet theory. Good agreement is obtained. The control concepts are straightforward and can be implemented with a minimum of hardware. Three-axis control accuracy on the order of one-half degree may be expected in typical applications.

Nomenclature

a	= semimajor axis of orbit
$\boldsymbol{B}$	= geomagnetic induction
B_ψ, B_ϕ, B_θ	= components of B
B_0	= equatorial field strength–defined by Eq. (18)
h	= spacecraft angular momentum in roll/yaw plane. For fine control analysis, with $I_\psi = I_\phi = 0$, h is the projection of the H_B vector on the roll/yaw plane. Note that $\beta H = h$
H	= spacecraft total angular momentum $(H_B + I \cdot \omega)$
H_B	= momentum bias
I_j	= j axis moment of inertia (assumed to be principal)
I_T	= transverse moment of inertia $= (I_\phi I_\psi)^{1/2}$
I_θ	= pitch moment of inertia
K_i	= various constants
M	= spacecraft dipole moment
M_{sat}	= maximum commandable dipole moment
P	= orbital period
s	= Laplace transform operator
T	= kinetic energy
t_n, t_0	= time constants
α	= nutation angle
β	= spin angle: angle between total angular momentum and orbit normal $(\psi^2 + \phi^2)^{1/2}$
λ	= orbit angle, measured from ascending node
ω	= spacecraft angular velocity with respect to inertial frame
ω_0	= orbital rate
ω_n	= angular frequency of nutation $[H_B/(I_\psi I_\phi)^{1/2}]$
ω_T	= transverse angular velocity associated with nutation
ψ, ϕ, θ	= Euler angles–yaw, roll, and pitch. Defined by 1-2-3 sequence from astrodynamic trajectory frame
τ	= applied torque

Presented as Paper 74-923 at the AIAA Mechanics and Control of Flight Conference, Anaheim, Calif., August 5-9, 1974; submitted August 26, 1974; revision received October 31, 1975. This work was funded by ITHACO, Inc. and NASA/GSFC. Valuable assistance from David Sonnabend is hereby acknowledged.

Index category: Spacecraft Attitude Dynamics and Control.

*Research Engineer.

†Consultant, Space Systems Division. Member AIAA.

I. Introduction

THE popularity of momentum bias spacecraft is due primarily to their ability to provide reasonably good attitude control (0.1-0.5°, all axes) using straightforward and relatively inexpensive attitude control hardware. (See, for example, Barbera and Jansz.[1]) Their advantages and disadvantages have been the subject of exhaustive discussion during the last several years. Suffice it to say that the most important feature of momentum bias designs is that their gryroscopic stiffness (and the resulting quarter-orbit coupling) obviates the requirements for a yaw attitude sensor. This is a highly desirable result, significantly reducing control system cost and complexity.

If one decides on a momentum bias design, there is still the matter of choosing a reaction torque source. Often, a mass expulsion system is chosen. Alternately, active magnetic techniques can be shown to have many advantages. These include their smooth continuous manner of operation (in contrast to the impulsive character of mass expulsion systems), essentially unlimited mission life (since no expendables are involved), and absence of catastrophic failure modes.

Magnetic control techniques have been the subject of a number of prior investigations.[2-12] Magnets have been used on many operational spacecraft including Nimbus, ERTS, ITOS, RAE, and OAO. In some cases (Nimbus & ERTS), the magnets are used to offset fixed imbalances, and are adjusted via ground commands. The ITOS system[2] uses magnets for precession control. However, the system is not autonomous; the magnets are controlled via ground commands. A closed-loop magnetic system is used to regulate reaction wheel momenta on the OAO.

In one of the first papers on magnetic attitude control, White et al.[3] sketched a closed-loop system and discussed its feasibility. Ergin and Wheeler[4] proposed an autonomous precession (pointing) control system using a pitch axis dipole. In a subsequent paper,[5] Wheeler used the method of averaging to improve upon his earlier control law. Renard[6] obtained an open-loop control law that requires quarter-orbit switching for near-polar orbits.

Sonnabend[7] and Dahl and Foxman[8] developed precession control laws that utilize a roll axis dipole. Tossman[9] appears to have been the first to consider active magnetic nutation and despin control, although the use of passive (hysteretic) magnetic schemes for these purposes was already well established. His scheme is based upon passive hysteresis rods.

In a comprehensive report, Sorenson[10] described a high-precision magnetic pointing system and compared its performance with and without a state estimator. Sorenson has included a rather complete bibliography of work performed prior to 1969. Stickler[11] has described a scheme that will despin a satellite subject to arbitrary initial tumbling. In addition, if the satellite is of the momentum bias variety, the same control laws provide for initial roll/yaw orientation.

In 1973, Collins and Bonello[12] discussed several possible autonomous magnetic control schemes that provide nutation as well as precession control.

In all of these systems, the last excepted, the magnetic control system is used only to provide precession control, and occasionally, for momentum regulation (i.e., spin rate or wheel speed control). Hence, a nutation damper and some sort of control system for accomplishing initial acquisition are still requireda magnetic attitude control system that would perform these additional functions, while providing precession control and momentum regulation, would be highly desirable. Collins and Bonello have suggested one implementation. Their proposal suffers somewhat from the circumstance that precession control is accomplished, essentially, by processing roll-rate information from a horizon scanner. Since the data could be very noisy, an alternate scheme might be worthwhile.

This paper describes and discusses a fully autonomous magnetic attitude control system that performs the following functions: 1) initial acquisition, 2) nutation damping, 3) precession control, and 4) momentum bias regulation. The system is best suited for low-altitude, high-inclination, Earth-pointing momentum-bias spacecraft. Designed for three-axis-control spacecraft, it could be used on spinning satellites with minor modification.

The system consists of three orthogonal electromagnets (mounted along the vehicle control axes), a three-axes magnetometer, and a Scanwheel‡. The Scanwheel performs two functions. It provides a pitch-axis momentum bias while measuring satellite pitch and roll attitude. Pitch control is accomplished in the usual way by driving the Scanwheel in response to (properly compensated) pitch attitude errors; the roll- and yaw-axis magnets are used to regulate the magnitude of the pitch momentum bias. Precession control and nutation damping are provided by driving the pitch-axis magnet with (properly compensated) horizon scanner and magnetometer signals. Initial attitude acquisition, from arbitrary tumbling conditions, is performed by driving the magnets in response to magnetometer signals. All functions are performed autonomously, with little need for mode switching.

The various functions of this control system are analyzed in the next section. Time constants, effectiveness factors, and transfer functions are obtained which permit one to estimate (and modify) system performance. These analytical expressions are then compared with numerical solutions of the governing differential equations. Lacking flight data, such solutions represent our best estimate of system performance, and permit an evaluation of the analyses—for at least one set of parameters.

In a final section, an estimate of the weight and power requirements of this system are provided.

II. Initial Acquisition

Despin from arbitrary initial tumbling is accomplished by commanding the i^{th} body axis dipole M_i according to

$$M_i = K\dot{B}_i \quad (i=1,2,3) \quad K>O \tag{1}$$

where $\dot{B}_i$ is the time derivative of the i^{th} body axis component of the geomagnetic field and K is a constant. Thus, the $\dot{B}_i$ may be obtained directly by differentiating the output of the body mounted magnetometers. This scheme was originally proposed by Seymor Kant, Peter Hui, and Marty Lidston of GSFC. Its efficacy can be ascertained by considering the kinetic energy of an arbitrary body due to rotation about its center of mass.

We have

$$\frac{d}{dt}(T) = \dot{T} = \boldsymbol{\tau}\cdot\boldsymbol{\omega} \tag{2}$$

where $\boldsymbol{\tau}$ is the external torque acting on the body. The torque on a dipole in a magnetic field is given by

$$\boldsymbol{\tau} = \boldsymbol{M}\times\boldsymbol{B} \tag{3}$$

From a basic theorem of kinematics we have

$$(d^{\text{inertial}}/dt)\ (\boldsymbol{B}) = (d^{\text{body}}/dt)\ (\boldsymbol{B}) + \boldsymbol{\omega}\times\boldsymbol{B}$$

Since $\boldsymbol{B}$ as observed in inertial axes, varies at angular rate $2\omega_0$, we have for $\omega >> 2\omega_0$

$$\dot{\boldsymbol{B}} \approx \boldsymbol{B}\times\boldsymbol{\omega} \tag{4}$$

where $\dot{\boldsymbol{B}}$ is measured, as in Eq. (1), relative to body fixed axes. Combining Eq. (2-4), we obtain

$$\dot{T} = \dot{\boldsymbol{B}}\cdot\boldsymbol{M} \tag{5}$$

Implementing the control policy [Eq. (1)], we see that

$$\dot{T} = K\dot{B}^2 = -K|\boldsymbol{B}\times\boldsymbol{\omega}|^2 \tag{6}$$

which is clearly less than or equal to zero.

Equation (6) shows that we cannot reduce the kinetic energy associated with the component of ω parallel to $\boldsymbol{B}$. This should be clear, since the magnetometer cannot sense this motion, nor can the magnets provide a torque along $\boldsymbol{B}$. Fortunately, the orbital motion of the satellite insures that the direction of $\boldsymbol{B}$ does not remain fixed. The net effect of the policy [Eq. (1)] is to eliminate all angular motion between the satellite and the field, resulting in a terminal motion such that the satellite is rotating once per orbit about the trajectory pitch axis.

Equation (6) indicates that T is proportional to T, so we might expect to see an exponential decay in ω. In practice, the gain K is quite large, the dipoles M_i are driven to saturation, and we see instead (to first order) a linear decrease in vehicle angular rates. [See Eq. (3), and let $\tau = M_{\text{sat}}\times B = \dot{H}$.] Since $\boldsymbol{B}$ and ω are not always perpendicular, the average time rate of change of vehicle angular momentum (in particular, that momentum associated with vehicle angular motion, and not that due to momentum wheels) is somewhat less than $\tau_{\max} = -BM_{\text{sat}}$. The ratio of these two quantities constitutes a measure of the effectiveness of the despin system. It is the author's observation that, for high-inclination orbits, this effectiveness lies in the range 0.50-0.80 for a wide range of system parameters (H_B, M_{sat},B,ω). Figure 1 shows how the momentum associated with the tumbling motion of a spacecraft is reduced by application of this control scheme. The average effectiveness factor for the case shown is about 0.65. These results and the "exact" results of Figs. 2-6 were obtained by numerical integration of the exact equations of motion (Euler's equations with momentum bias added).

If the spacecraft is of the momentum-bias variety, this same control law [Eq. (1)] will force a terminal attitude such that the vehicle pitch axis aligns with the orbit normal. (A subsequent rotation about the pitch axis is, then, all that is required for initial acquisition.) This orientation is the only one in which the spacecraft may "lock-up" with the Earth's field without the application of a large body-fixed roll/yaw torque. The behavior is analogous to the gyrocompass of a ship; the magnetic control system opposes relative motion between the field and spacecraft, just as the viscous fluid in a

‡Scanwheel is a registered trademark of ITHACO, Inc.

gyrocompass damps relative motions in that system, resulting in alignment between the gyrocompass axis and the spin axis of the Earth.

A linearized stability analysis indicates (see Stickler[11]), and numerical solutions confirm, that for this terminal attitude motion to be stable we must have

$$H_B + 2I_\theta\omega_0 > 2I_T\omega_0 \tag{7}$$

The factor $2\omega_0$ appears in Eq. (7) because the acquisition control system reduces the spin rate to twice orbital rate, i.e., $2\omega_0$. For a practical system, the author recommends that the inequality (7) be exceeded by a factor of three or more. Figure 2 shows how the angle between the orbit normal and the vehicle pitch axis β is reduced during this phase of acquisition. Again, the data were obtained by numerically solving the equations of motion. Once acquisition is achieved the control mode should be switched to the on-orbit control mode.

An effectiveness factor for this orientation maneuver can be defined analogously with the despin effectiveness factor

$$E \equiv \dot{\beta}H_B / BM_{\theta,\text{sat}} \tag{8}$$

One observes that E decreases as β decreases. E lies in the neighborhood of 0.75 for $\beta > 30$ deg, is about 0.50 for $\beta \cong 10$ deg, and drops to about 0.20 for $\beta < 10$ deg. Using these factors one can obtain a rough idea of the time required for initial acquisition.

III. On-Orbit Control

In the on-orbit fine control mode the roll- and yaw-axis dipoles are used to regulate the pitch momentum bias, while the pitch-axis dipole provides roll/yaw attitude control. Reaction wheel control of the pitch loop is assumed. The analysis given here is based on three main assumptions: 1) the geomagnetic field may be modeled as a dipole, 2) the spacecraft is in a magnetic polar orbit, and 3) nutational and orbital oscillations may be decoupled, by virtue of their frequency separation. The analysis by Alfriend[13] shows that the nutational and orbital oscillations can be decoupled.

Momentum Unloading

The momentum unloading strategy is quite simple and was, in fact, proposed 13 years ago by White et al.[3] One should set

$$M = -K_u B \times (H - H_B) \tag{9}$$

to reduce the overall momentum error. In our case, this amounts to

$$M_\psi = -K_u B_\phi \Delta h \quad M_\phi = K_u B_\psi \Delta h \tag{10}$$

where Δh is the pitch momentum error. K_u is typically sized to command full dipole strength for a 10% momentum error. Using 10 Am^2 electromagnets, and the parameters listed in Figure 2, one could unload about 2 N-m-sec of momentum/orbit from the pitch axis.

Pointing Control

Precession (pointing) control and nutation damping are provided by driving the pitch-axis dipole according to

$$M_\theta = K_1 B_\phi \phi - K_2 \dot{B}_\theta \tag{11}$$

The first term provides precession control, the second nutation damping. It will be shown that the $K_1 B_\phi \phi$ term pumps energy into the nutation mode, while the $-K_2\dot{B}_\theta$ term damps nutation; there is a critical ratio K_1/K_2 necessary to insure stability.

If the nutational and orbital modes of vehicle response are assumed to be decoupled, the equations governing these motions become more tractable. Comparisons of analyses using the method of multiple time scales (see Alfriend[13]) and numerical solutions (Floquet theory and simulation) indicate that worthwhile results may be obtained on this basis.

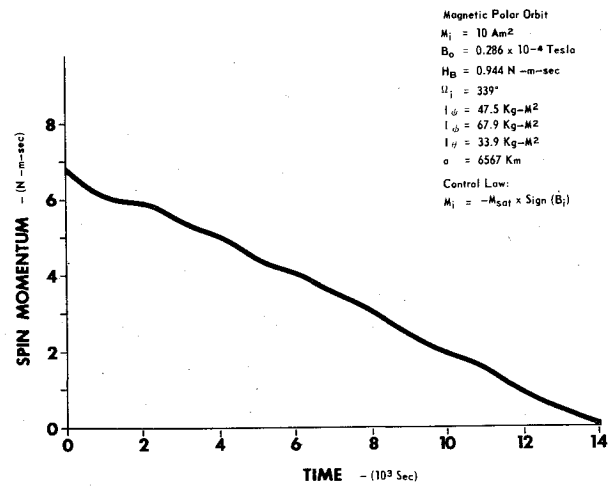

Fig. 1 Initial despin.

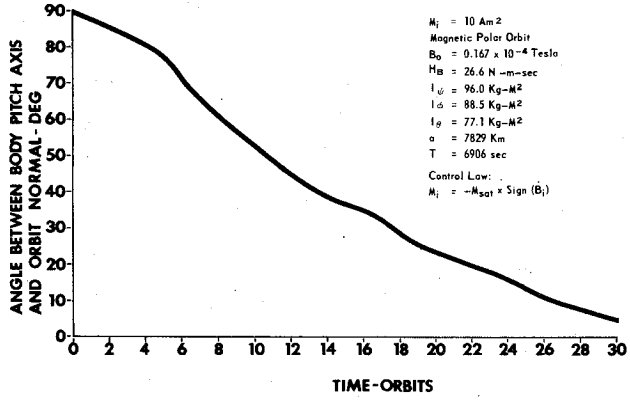

Fig. 2 Spin axis orientation.

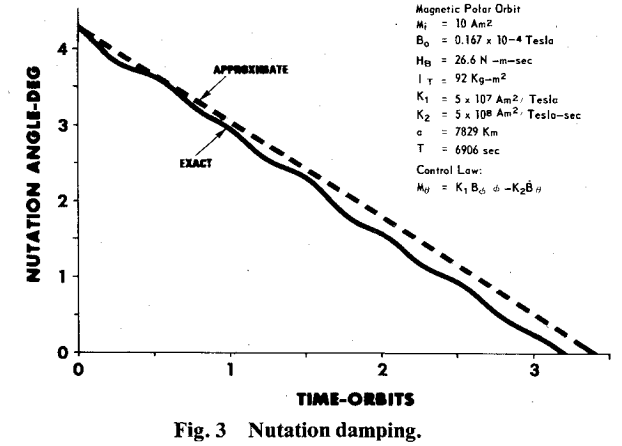

Fig. 3 Nutation damping.

Nutation Damping

For small attitude errors, we have

$$\dot{B}_\theta = B_\psi\dot{\phi} - B_\phi\dot{\psi} \tag{12}$$

The nutation damping term in Eq. (11) ($-K_2\dot{B}_\theta$) generates control torques given by

$$\tau_\psi = -K_2B_\phi^2\dot{\psi} + K_2B_\psi B_\phi\dot{\phi} \quad \tau_\phi = -K_2B_\psi^2\dot{\phi} + K_2B_\phi B_\psi\dot{\psi} \tag{13}$$

which are clearly of the correct sign. For large K_2, and an appreciable nutation angle α, M_θ will be full on and of polarity such that τ lies in the halfplane opposite ω. Averaging $\tau \cdot \omega/\omega$ over one nutation cycle, we obtain the effective control torque for nutation damping. Assuming the pitch-axis dipole to be full on over the entire cycle, we compute

$$\dot{\alpha} H_B = (2/\pi) B M_{\theta,\text{sat}} \tag{14}$$

Figure 3 shows how this scheme works in practice. The parameters chosen are similar to those of the ITOS spacecraft. Figure 3 shows that Eq. (14) is a good approximation for the nutation damping during saturation.

For nutation angles small enough so that the pitch-axis dipole is not saturated, Eq. (13) shows that the damping torques are proportional to the nutation amplitude. Averaging $\tau \cdot \omega/\omega$ over one nutation period, as before, and remembering

$$\omega_n = H_B/(I_\psi I_\phi)^{1/2}, \quad \omega_T = \omega_n \alpha$$

one finds that

$$\dot{\alpha} = -K_2 B^2 \alpha / 2 I_T \tag{15}$$

so that we have linear nutation damping with time constant t_n given by

$$t_n = 2 I_T / K_2 B^2 \tag{16}$$

For the parameters listed in Fig. 3, and an average value of $B^2 = 2.5 B_0^2$, we compute $t_n = 530$ sec.

If $K_1 \neq 0$ [see Eq. (11)], these statements need to be modified; this point will now be discussed further.

Precession Control

Next, we proceed to investigate spacecraft orbital mode oscillations. Expressions for responses to initial attitude errors are presented first. Subsequently, approximate transfer functions, indicating responses to various perturbing forces are developed and compared with numerical solutions.

Transient response

Orbital mode oscillations are controlled by the first term in Eq. (11), $K_1 B_\phi \phi$, which generates control torques

$$\tau_\phi = K_1 B_\psi B_\phi \phi \quad \tau_\psi = -K_1 B_\phi^2 \phi \tag{17}$$

In accordance with the previously stated assumptions regarding the geomagnetic field and orbit, we have, for small ψ and ϕ

$$B_\psi = -2B_0 \sin\lambda \quad B_\phi = B_0 \cos\lambda \quad B_\Theta = 0 \quad \lambda = \omega_0 t \tag{18}$$

where λ is the orbit angle, measured from the ascending node.

To decouple short-term responses (i.e., nutation), set $I_\psi = I_\phi = 0$. The resultant equations of motion describe the precession of the momentum-bias vector $\boldsymbol{H}_B \approx \boldsymbol{H}$. A study of the spacecraft attitude thus reduces to a study of the components of $\boldsymbol{H}_B$ projected on the orbit plane. If we denote these projections along the trajectory§ yaw and roll axes by h_ψ and h_ϕ, the equations of motion, in rotating trajectory axes, are

$$\dot{h}_\psi = \omega_0 h_\phi + \tau_\psi \quad \dot{h}_\phi = -\omega_0 h_\psi + \tau_\phi \tag{19}$$

A first-order analysis of the response for various initial conditions can be obtained by assuming that the effect of the control torques [Eq. (17)] over a half-orbit is small. Hence, quarter-orbit coupling implies that

$$h_\psi = h_\psi^0 \cos\lambda + h_\phi^0 \sin\lambda \quad h_\phi = h_\phi^0 \cos\lambda - h_\psi^0 \sin\lambda \tag{20}$$

§Trajectory yaw and roll axes are the axes defined by the body yaw and roll axes when $\psi = \phi = 0$.

The superscript denotes values at the ascending node. Eq. (20) allows us to obtain an expression for the control torques [Eq. (17)] in terms of the yaw and roll errors at the ascending node ψ^0 and ϕ^0, since we know

$$\phi = h_\psi / H \quad \psi = h_\phi / H \tag{21}$$

Next, suppose we write $\tau = \dot{h}$ with $\tau \neq \tau_\psi \hat{i} + \tau_\phi \hat{j}$ [Eq. (17)] and $h = h_\psi \hat{i} + h_\phi \hat{j}$ [Eq. (20)]. Noting that the pointing error

$$\beta = (\psi^2 + \phi^2)^{1/2}$$

that $\beta H = h$, and that

$$d/dt\,(h) = \dot{\beta} H = \tau \cdot h / h \tag{22}$$

one can show

$$\tau \cdot h / h^2 = \dot{\beta} / \beta \tag{23}$$

Evaluating the quantity on the left with the aid of [Eq. (18)], we obtain

$$\frac{\dot{\beta}}{\beta} = \frac{-K_1 B_0^2}{H} \left[a_1 \left(\frac{1}{1+x^2} \right) + a_2 \left(\frac{x^2}{1+x^2} \right) + a_3 \left(\frac{x}{1+x^2} \right) \right] \tag{24}$$

$$a_1 = (3/4)\sin^2 2\lambda \quad a_2 = \cos^2\lambda (3\cos^2\lambda - 2)$$

$$a_3 = \sin 2\lambda (3\cos^2\lambda - 1) \quad x = (h_\psi^0 / h_\phi^0) = -\phi^0/\psi^0$$

For the case $\phi^0 = 0$, only the first term in Eq. (24) remains. Averaging over one orbit, we have

$$\dot{\beta} = -(3/8)\,(K_1 B_0^2 / H)\beta \tag{25}$$

which indicates that β decays exponentially with time constant $8H/3K_1B_0^2$. Note that $\dot{\beta}$ varies as $\sin 2\lambda$, so that $\dot{\beta} = 0$ at the orbital nodes and poles and takes on a maximum at middle latitudes. On the other hand, as ψ^0 approaches 0, only the second term of Eq. (24) remains. Again averaging over one orbit

$$\dot{\beta} = -(1/8)\,(K_1 B_0^2 / H)\beta \tag{26}$$

so that the time constant associated with this mode of oscillation is three times the one corresponding to $\phi^0 = 0$. Also, note that $\dot{\beta} < 0$ only for $3\cos^2\lambda > 2$, i.e., within about 35 deg of the magnetic equator. In view of this circumstance, it has been proposed that we either set $K_1 = 0$ or change its sign above a specified (magnetic) latitude. The effect of such schemes may be evaluated by averaging Eq. (24) over an orbit; if we set $K_1 = 0$ above 50 deg (magnetic) latitude the time constants for the two modes become equal at about

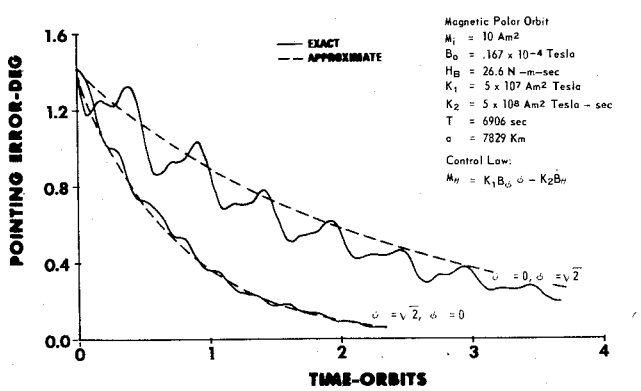

Fig. 4 Transient response.

$$t_0 = 4.5H/K_1B_0^2$$

The time constants predicted in this analysis agree with those predicted by more rigorous analyses (Alfriend[13]) if we replace K_1 with $K_1 + 2\omega_0 K_2$. Of course, the best way to check the validity of this analysis (lacking flight data) is to compare it with numerical solutions of the governing equations. Application of Floquet theory (a numerical procedure) to the system, for the parameters listed in Figure 4, yields time constants within 15% of those indicated by Eqs. (25) and (26). Figure 4 shows the system response in the two modes. One can see that agreement with the analysis just given is quite good.

Stability

As mentioned earlier, the precession control law tends to excite nutation. This can be seen by considering the fact that, during nutation, the vectors $\boldsymbol{h}$ and $\boldsymbol{I}\cdot\boldsymbol{\omega}$ are oppositely directed and of equal magnitude. Since the torque due to the precession control law is directed, on net, opposite $\boldsymbol{h}$ it has a projection along $\boldsymbol{\omega}$. For any given K_1, a minimum value of K_2 is required to insure stability. Using an energy approach, one finds that the requirement is

$$K_2 > (1/\omega_n)\ (B_\phi^2/B^2)K_1 \tag{27}$$

The inequality is a function of orbital position, as shown by Eq. (18), and is most restrictive at the nodes, where $B_\phi = B$. As a function of the field components the nutation time constant is given by

$$t_n = 2I_T/(K_2B^2 - K_1B_\phi^2/\omega_n) \tag{28}$$

And the requirement for stability is $t_n > 0$.

Forced response

The response of this system to disturbances is obtained by examining the equations of motion [Eq. (19)] with disturbance torques τ_ψ and τ_ϕ added to the control torques [Eq. (17)]. Substituting in Eqs. (21) and (18), we have

$$\phi' + (K^*\cos^2\lambda)\phi + \psi = \tau_\psi/H\omega_0 \tag{29a}$$

$$\psi' - (1 + k^*\sin 2\lambda)\phi = -\tau_\phi/H\omega_0' \equiv d/d\lambda \tag{29b}$$

$$K^* = K_1B_0^2/H\omega_0 \tag{29c}$$

Even for the case $\tau_\psi = \tau_\phi = 0$, the authors are unable to obtain a closed-form solution to Eq. (29). However, for small values of K^*, we may obtain an approximate solution in several ways. With the average values of the time varying coefficients, Eq. (29) corresponds to a damped second-order system with natural frequency ω_0 and damping ratio $\xi = K^*/4$. The system has transfer functions

$$\psi/\tau_\psi = \phi/\tau_\phi = (1/H\omega_0)/\Delta \tag{30a}$$

$$\psi/\tau_\phi = -[s/H\omega_0 + K^*/2H\omega_0]/\Delta \tag{30b}$$

$$\phi/\tau_\psi = (s/H\omega_0)/\Delta \quad \Delta = s^2 + (K^*/2)s + 1 \tag{30c}$$

For *constant* roll and yaw disturbances τ_ϕ and τ_ψ, Eqs. (30) predict steady-state solutions

$$\phi = \tau_\phi/H\omega_0 \quad \psi = -\tau_\phi K^*/2H\omega_0 \quad (\tau_\psi = 0, \tau_\phi = \text{const.}) \tag{31}$$

while for $\tau_\psi = \text{const.}$, $\tau_\phi = 0$

$$\phi = 0 \quad \psi = \tau_\psi/H\omega_0 \tag{32}$$

Note that the direct responses (ϕ/τ_ϕ and ψ/τ_ψ) are independent of gain, while ψ/τ_ϕ actually increases with K^*.

The greatest difficulties, however, are due to torques, generated by a residual pitch-axis dipole. These torques vary sinusoidally at orbit rate and excite the system near resonance. Since they have a secular component (in inertial coordinates), if we had no control ($K_1 = 0$), the pointing error would increase indefinitely.

Using Eq. (30), one can show that the steady-state roll and yaw errors corresponding to a residual pitch dipole of strength M are

$$\phi = (2M/K_1B_0)\cos\lambda \quad \psi = (2M/K_1B_0)\sin\lambda - K^*\cos\lambda) \tag{33}$$

A more rigorous analysis by Alfriend[13] using the method of multiple time scales, yields results identical to those given in Eqs. (31) and (32), except that in evaluating K^*, K_1 must be replaced by $K_1 + 2\omega_0 K_2$. He found, however, the response to a pitch-axis dipole to be *twice* that given by Eq. (33). This difference may be attributed to the fact that the coefficients in Eq. (29) are varying at frequency $2\omega_0$, while the torques generated by the dipole vary at ω_0. Averaging the coefficients is not permissible under these circumstances. In any case, note that the response does not depend on H.

The above expressions may be compared with solutions obtained by numerically integrating the governing equations. Figure 5 shows the pointing error, $\beta = (\psi^2 + \phi^2)^{1/2}$ for a 2.5 Am^2 residual pitch dipole. For the parameters listed, Alfriend's analysis predicts

$$\beta = 0.74[1 + 0.52\sin(2\lambda + \gamma)]^{1/2}\text{deg}$$

γ is a phase angle. Figure 5 shows this estimate to be about 20% too high. Figure 6 shows the solution for β correspon-

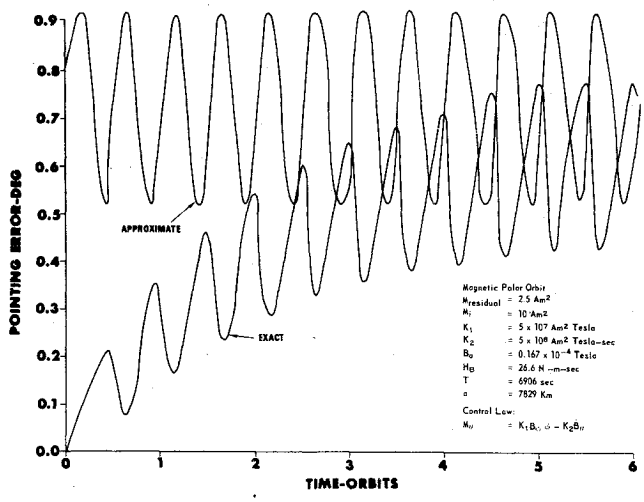

Fig. 5 Response to residual pitch dipole.

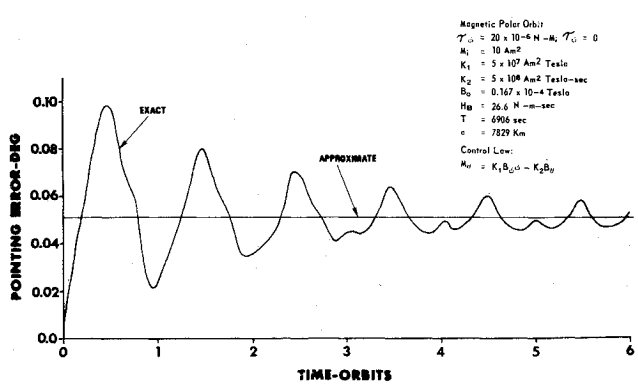

Fig. 6 Response to constant roll torque.

ding to a constant roll torque of 20×10^{-6}N-m. The steady-state response is in excellent agreement with Eqs. (31), which predict $\beta = 0.051$ deg.

Based on the results presented here, and on a number of numerical solutions, the authors recommend choosing a value of K^* in the range $1 < K^* < 3$, depending on the particular disturbance environment anticipated.

IV. Conclusions

A conceptually straightforward scheme for the autonomous control of momentum bias spacecraft has been proposed. Signals from a horizon scanner and three-axis magnetometer are used to control the strength of three orthogonal electromagnets. The control system provides for initial acquisiton, nutation damping, and pointing control. The control laws are elementary; their implementation requires a minimum of hardware.

Analyses of the various phases of operation indicate the following: In the despin phase, spin angular momentum is removed at a (roughly) constant rate. Similarly, large angle nutation decays linearly [as shown by Eq. (14)]. Small-amplitude nutation decays exponentially with a time constant predicted by Eq. (16). After the spacecraft has been despun, the acquisiton control law provides initial roll/yaw stabilization.

When initial stablilzation has been completed, only the pitch-axis dipole is required for pointing control and nutation damping. Bias momentum regulation is provided by the roll- and yaw-axis dipoles. Expressions characterizing transient and forced responses were obtained, along with a stability criterion. These expressions, obtained from a straightforward application of first principles, were compared with expressions determined using the method of multiple time scales, with Floquet theory, and with direct numerical solutions. Good agreement was obtained in most cases. Predicted attitude errors are a function of anticipated disturbances; in typical applications we would expect errors of the order of 0.5 deg (all axes).

In summary, the authors believe that this control concept represents a low-cost, reliable, light-weight design appropriate for many Earth observatory spacecraft. We estimate, for example, that a system with the parameters listed in Figs. 2-5 would weigh less than 30 lb and require about 15 W.

References

[1] Barbera, F.J. and Jansz, J., "The Design of a Two-Wheel Momentum-Bias System for the Attitude Control of Spacecraft in Low-Altitude Orbits," AIAA Paper N.73-855, Key Biscayne, Fla., 1973.

[2] Lindorfer, W. and Muhlfelder, L., "Attitude and Spin Control for TIROS Wheel," AIAA/JACC Guidance and Control Conference Papers, Seattle, Wash., Aug. 1966, pp. 448-461.

[3] White, J.S., Shigemoto, F.H., and Bourquin, K., "Satellite Attitude Control Utilizing the Earth's Magnetic Field," NASA TN-D1068, Aug. 1961.

[4] Ergin, E.I. and Wheeler, P.C., "Magnetic Attitude Control of a Spinning Satellite," *Journal of Spacecraft and Rockets*, Vol. 2, Nov.-Dec. 1965, pp. 846-850.

[5] Wheeler, P.C. "Spinning Spacecraft Attitude Control via the Environmental Magnetic Field," *Journal of Spacecraft and Rockets*, Vol. 4, Dec. 1967, pp. 1631-1637.

[6] Renard, M.L. "Command Laws for Magnetic Attitude Control of Spin-Stabilized Earth Satellites," *Journal of Spacecraft and Rockets*, Vol. 4, Feb. 1967, pp. 156-163.

[7] Sonnabend, D. "A Magnetic Control System for an Earth-Pointing Satellite," *Proceedings of the Symposium on Attitude Stabilization and Control of Dual-Spin Spacecraft,*" Aug. 1967, Aerospace Rept. TR-0158 (3307-01)-16.

[8] Dahl, P.R. and Foxman, E., "Automatic Magnetic Attitude Control for a Wheelbarrow Spacecraft," Aerospace Rept. TR-0158 (3113-03)-1, Sept. 1967.

[9] Tossman, B.E. "Magnetic Attitude Control System for the Radio Astronomy Explorer-A Satellite," *Journal of Spacecraft and Rockets*, Vol. 6, March 1969, pp. 239-244.

[10] Sorenson, J.A. *Precision Magnetic Attitude Control of Spinning Spacecraft*, Stanford Univ. Stanford, Calif., SUDAAR 380, Aug. 1969.

[11] Stickler, A.C., "A Magnetic Control System for Attitude Acquisition," ITHACO, Inc., Ithaca, N.Y., Rept. 90345, Jan. 1972.

[12] Collins, D.H. and Bonello, D.P., "An Attitude Control System for Earth Observation Spacecraft," AIAA Paper 73-854, Key Biscayne, Fla., 1973.

[13] Alfriend, K.T. "A Magnetic Attitude Control System for Dual-Spin Satellites," *AIAA Journal*, Vol. 13, June 1975, pp. 817-822.